



■ BONE BIOLOGY

Effects of interfacial micromotions on vitality and differentiation of human osteoblasts

**J. Ziebart,
S. Fan,
C. Schulze,
P. W. Kämmerer,
R. Bader,
A. Jonitz-Heincke**

Rostock University
Medical Center,
Rostock, Germany

■ J. Ziebart, M.Sc., Research Assistant, Department of Orthopaedics,
■ S. Fan, Research Assistant, Department of Orthopaedics,
■ C. Schulze, M.Sc., Research Assistant, Department of Orthopaedics,
■ P. W. Kämmerer, Dr. med. habil. Dr. med. dent., Deputy Director, Department of Oral, Maxillofacial and Plastic Surgery,
■ R. Bader, Prof. Dr. med. habil. Dipl.-Ing., Professor for Biomechanics and Implant Technology, Head of Research Laboratory, Department of Orthopaedics,
■ A. Jonitz-Heincke, Dr. rer. hum., Deputy Head of Research Laboratory, Department of Orthopaedics, Rostock University Medical Center, Rostock 18057, Germany.

Correspondence should be sent to A. Jonitz-Heincke;
email: anika.jonitz-heincke@med.uni-rostock.de

doi: 10.1302/2046-3758.72.BJR-2017-0228.R1

Bone Joint Res 2018;7:187–195.

Objectives

Enhanced micromotions between the implant and surrounding bone can impair osseointegration, resulting in fibrous encapsulation and aseptic loosening of the implant. Since the effect of micromotions on human bone cells is sparsely investigated, an *in vitro* system, which allows application of micromotions on bone cells and subsequent investigation of bone cell activity, was developed.

Methods

Micromotions ranging from 25 μm to 100 μm were applied as sine or triangle signal with 1 Hz frequency to human osteoblasts seeded on collagen scaffolds. Micromotions were applied for six hours per day over three days. During the micromotions, a static pressure of 527 Pa was exerted on the cells by Ti6Al4V cylinders. Osteoblasts loaded with Ti6Al4V cylinders and unloaded osteoblasts without micromotions served as controls. Subsequently, cell viability, expression of the osteogenic markers collagen type I, alkaline phosphatase, and osteocalcin, as well as gene expression of osteoprotegerin, receptor activator of NF- κ B ligand, matrix metalloproteinase-1, and tissue inhibitor of metalloproteinase-1, were investigated.

Results

Live and dead cell numbers were higher after 25 μm sine and 50 μm triangle micromotions compared with loaded controls. Collagen type I synthesis was downregulated in respective samples. The metabolic activity and osteocalcin expression level were higher in samples treated with 25 μm micromotions compared with the loaded controls. Furthermore, static loading and micromotions decreased the osteoprotegerin/receptor activator of NF- κ B ligand ratio.

Conclusion

Our system enables investigation of the behaviour of bone cells at the bone-implant interface under shear stress induced by micromotions. We could demonstrate that micromotions applied under static pressure conditions have a significant impact on the activity of osteoblasts seeded on collagen scaffolds. In future studies, higher mechanical stress will be applied and different implant surface structures will be considered.

Cite this article: *Bone Joint Res* 2018;7:187–195.

Keywords: Micromotion, Osteoblast, Osteoblast differentiation, Osseointegration, Endoprosthesis

Article focus

- To investigate the effect of micromotions on the viability of human osteoblasts.
- To investigate how micromotions influence the activity of human osteoblasts.

Key messages

- A novel *in vitro* system for application of micromotions up to 100 μm was tested on human osteoblasts.
- 25 μm sine micromotions increased live cell numbers and affected osteoblast

differentiation by decreasing collagen type I synthesis rates and by increasing osteocalcin transcripts.

- Micromotions reduced osteoprotegerin/receptor activator of NF- κ B ligand ratio in human osteoblasts.

Strengths and limitations

- This study reveals how shear stress, induced by micromotions of an implant, affects function of human osteoblasts and therefore influences osseointegration.

- In the presented *in vitro* system, strategies can be tested that promote activity of bone cells when faced with micromotions.
- In the presented *in vitro* system, it is not possible to exert a dynamic pressure on bone cells during application of micromotions. In the experiments, a polished titanium surface was used rather than a stochastically rough or geometric surface structure.

Introduction

Cementless total hip arthroplasty (THA) is increasingly performed, especially for younger patients demanding high mobility.^{1,2} Excellent osseointegration of the endoprosthesis is critical for long-term stability and survival outcome. Osseointegration is defined as the process leading to a direct contact between the bone and the load-bearing implant that form a structural and functional unit without the interposition of fibrous tissue and relative progressive movement of the implant in the bone stock.^{3,4} The process involves an inflammatory, proliferative, and remodelling phase during which a callus is formed, subsequently replaced by immature woven bone, and finally converted into lamellar bone.⁵ Osseointegration is influenced by: the implant design; surface structure and properties; status of press fit; intrinsic factors, including status of host bed, regenerative capacity, or medical condition; and extrinsic factors, such as medication, radiation, physical stimulation, and loading conditions.⁶⁻¹³ If osseointegration is not sufficient, micromotions of the implant relative to the surrounding bone tissue can occur. Enhanced micromotions result in fibrous encapsulation of the implant and facilitate aseptic loosening, making revision surgery necessary.

Amplitudes of micromotions that promote or prevent osseointegration are widely discussed in the literature.¹⁴⁻¹⁹ It has been shown that interfacial micromotions of less than 30 μm do not interfere with osseointegration, while micromotions larger than 40 μm can impair osseointegration, resulting in the formation of fibrous tissue and fibrocartilage at the bone-implant interface and hypertrophy of the surrounding trabecular bone.^{14,16-18} In line with these findings, Duyck et al¹⁹ showed a lower bone-implant contact when micromotions greater or equal to 30 μm were applied. Micromotions of an implant act on bone cells by exerting pressure and shear stress forces.²⁰ The impact of shear stress on orientation of osteoblast cell clusters, cell morphology, and elongation has been previously reported.²¹ To gain a better understanding of how micromotions influence bone cell activity, an *in vitro* system, which allows application of defined micromotions in a range of 0 μm to 100 μm under static pressure loading conditions, was developed. To approach the activity pattern of patients who underwent total joint arthroplasty, micromotions were applied for six hours a

day with a frequency of 1 Hz, which represents a normal gait cycle.

Materials and Methods

Experimental set-up. The system for application of micromotions consists of two parts (Fig. 1). The lower component supports the linear piezo positioning system. On top of the positioning system, a specific holder for a six-well plate is fixed. The upper part of the positioning system holds six slight bearings in which pins linked with highly polished titanium alloy (Ti6Al4V) cylinders are suspended. The cylinders, scaling 30 mm in diameter and 8 mm in height, rest on the bottom of each well with a static pressure load of 527 Pa resulting from the cylinder dimensions. The dimensions of the Ti6Al4V cylinders cover most of the bottom of the well while permitting gas exchange, micromotions, and moderate displacement of the medium. The linear piezo positioning system moves the six-well plate containing the human osteoblasts against the Ti6Al4V cylinders. The following micromotions were applied for six hours per day with a frequency of 1 Hz: 25 μm sine, 50 μm sine, 100 μm sine, and 50 μm triangle micromotions. The sine and triangle waveforms are depicted in Figure 2 for 50 μm micromotions applied with a frequency of 1 Hz. The linear piezo positioning system displaces the six-well plate 50 μm linear in one direction and 50 μm back to the original position within one second. The maximum velocities and accelerations resulting from the applied micromotions are shown in the table in Figure 2. The mean accuracy of micromotions ranging from 20 μm to 100 μm determined prior to the present study was -2.46% (SD 1.03) for sinusoidal micromotions and -4.55% (SD 1.47) for triangle micromotions due to the inertia of the system.

Human osteoblasts were isolated from the femoral heads of patients undergoing THA after the approval of the Local Ethical Committee (A 2010-10) and agreement from the patients, as previously described.²² Briefly, the spongiosa was digested with collagenase A and dispase II (Roche, Basel, Switzerland) for three hours at 37°C. The cell suspension was filtered and the isolated cells expanded in Dulbecco's Modified Eagle Medium (DMEM) without calcium, containing 10% fetal calf serum, 1% N-2-hydroxyethylpiperazine-N-2-ethane sulfonic acid (HEPES) buffer, 2.5 $\mu\text{g}/\text{ml}$ amphotericin B, and 100 U/ml penicillin/streptomycin under standard cell culture conditions. The medium was enriched with 10 mM β -glycerophosphate, 50 $\mu\text{g}/\text{ml}$ ascorbic acid, and 100 nM dexamethasone for osteogenic differentiation during cell cultivation and experiments. Donor cells used in cell experiments were obtained from five females (mean age 70.8 years (SD 11.5)) and four males (mean age 61.3 years (SD 12.1)). Donors were chosen randomly with regard to age and gender. Where possible, the same donors were used for different experimental parameters.

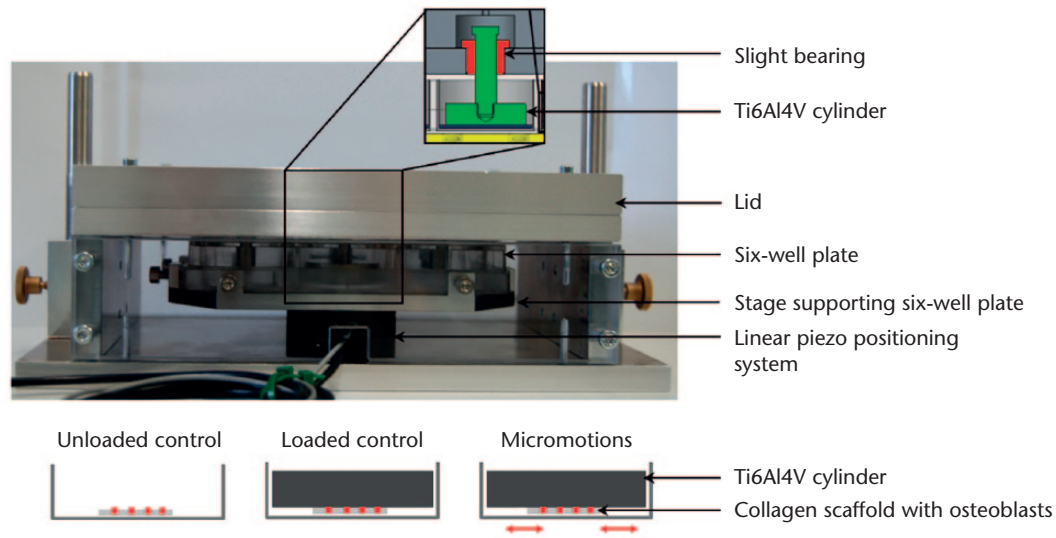


Fig. 1

System for application of micromotions. The stage supporting the six-well plate is fixed on top of the linear piezo positioning system. The lid of the system holds the titanium alloy (Ti6Al4V) cylinders mounted on slight bearings and resting on the samples. There are three experimental groups: osteoblasts seeded on collagen scaffolds (unloaded control); Ti6Al4V cylinders resting on collagen scaffolds with osteoblasts under static loading conditions (loaded control); and the six-well plate containing collagen scaffolds with osteoblasts, which is moved by the linear positioning system relative to static Ti6Al4V cylinders (micromotions, 25 μm to 100 μm).

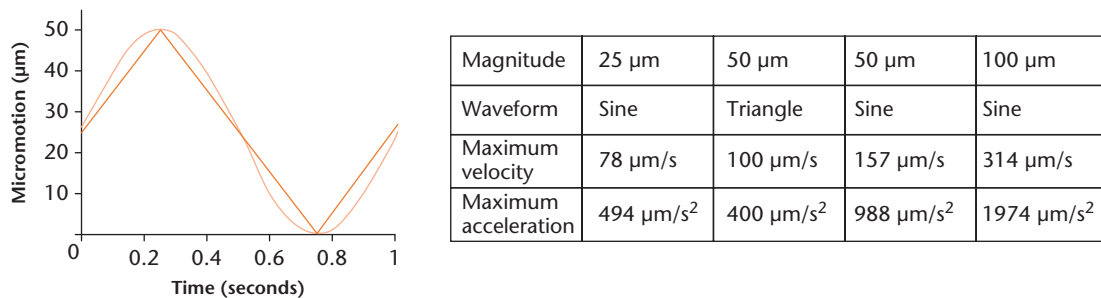


Fig. 2

Characteristics of applied micromotions. Depiction of a 50 μm sine (light orange function) and 50 μm triangle (dark orange function) micromotion applied with 1 Hz frequency. The table shows the maximum velocity and maximum acceleration of the applied micromotions resulting from the magnitude and waveform of the micromotions applied with 1 Hz frequency.

Collagen scaffolds of bovine origin (MedSkin Solutions Dr. Suwelack AG, Billerbeck, Germany), measuring 16 mm in diameter and 1 mm in height, were bonded to the well bottoms with a biocompatible silicon paste (Korasilon; Kurt Obermeier GmbH & Co. KG, Bad Berleburg, Germany); 1×10^5 cells in the third passage of culture were seeded on top of the collagen material. The following day, the lid of the cell culture plate was removed and the plate was placed into the system for micromotions so that Ti6Al4V cylinders rested on the collagen scaffolds. Micromotions differing in magnitude and waveform, as described above, were applied to osteoblasts for a total of three days. Osteoblasts on collagen scaffolds without loading (unloaded control) and osteoblasts loaded with static compression by the weight of the Ti6Al4V cylinders (loaded control) served as controls (Fig. 1). Loaded samples were chosen as reference samples because application of micromotions always involves

combined compression-tension loading of the samples. Furthermore, it represents the initial situation in the bone where a press-fit implanted endoprosthesis exerts a constant pressure to the surrounding bone.

Cell biological and molecular methods. For assessment of cell viability, the collagen scaffolds were transferred to a new well plate and the cells growing on the collagen material were stained with a Live/Dead assay kit (Life Technologies Corp., Carlsbad, California). Fluorescent images were taken with a Nikon Eclipse 120 fluorescence microscope (Nikon Instruments, Tokyo, Japan). The metabolic activity was measured by water soluble tetrazolium (WST-1) assay (Cell Proliferation Reagent; Roche, Basel, Switzerland) by incubation of the collagen material with WST-1 reagent diluted 1:10 in cell culture medium. In order to quantify the living cells, the collagen scaffolds were digested in collagenase A for one hour. The living cells were counted after Trypan blue

Table I. Primer sequences of osteogenic genes

HPRT	Forward Primer: 5'-CCCTGGCGTCGTGATTAGTG-3' Reverse Primer: 5'-TCGAGCAAGACGTTTCAGTCC-3'
COL1A1	Forward primer: 5'- ACGAAGACATCCCAACATC -3' Reverse primer 5'- AGATCACGTCATCGACAAC -3'
ALP	Forward primer: 5'- CATTGTGACCACCACGAGAG -3' Reverse primer 5'- CCATGATCACGTCATGTCC -3'
OC	Forward primer: 5'- TCAGCCAACTCGTCACAGTC -3' Reverse primer 5'- GGTGCAGCCTTTGTGTCC -3'
MMP-1	Forward primer: 5'- AGAGCAGATGTGGACCATGC -3' Reverse primer 5'- TCCCGATGATCTCCCCTGAC -3'
TIMP-1	Forward primer: 5'- ATTGCTGGAAAAGTGCAGGATG -3' Reverse primer 5'- GTCCACAAGCAATGAGTGCC -3'
OPG	Forward primer: 5'- AGGCATATTCTCTGTGCC -3' Reverse primer: 5'- GATGTCCAGAAACACGAGCG -3'
RANKL	Forward primer: 5'- TCTTCTATTTTCAGAGCCGAGATGG-3' Reverse primer 5'- CTGATGTGCTGTATCCAACG-3'

HPRT, hypoxanthine guanine phosphoribosyltransferase; COL1A1, collagen type I; ALP, alkaline phosphatase; OC, osteocalcin; MMP-1, matrix metalloproteinase-1; TIMP-1, tissue inhibitor of metalloproteinase-1; OPG, osteoprotegerin; RANKL, receptor activator of NF- κ B ligand

staining of the resulting cell suspension to discriminate between live and dead cells. Due to the very low number of dead cells counted after collagen digestion, the Live/Dead staining images were used for quantification of the dead cells by counting the red fluorescing nuclei using the open source image processing program ImageJ (NIH, Bethesda, Maryland).

Afterwards, the osteoblasts were lysed in TriReagent (Zymo Research, Irvine, California) and total RNA was extracted using the Direct-zol RNA MiniPrep Kit (Zymo Research). Reverse transcription of messengerRNA (mRNA) was done with the High Capacity cDNA Reverse Transcription Kit (Applied Biosystem, Foster City, California) following the manufacturer's instructions, and a semi-quantitative real-time polymerase chain reaction was performed in triplicates using innuMIX qPCR MasterMix SyGreen (Analytik Jena AG, Jena, Germany) for collagen type I (COL1A1), alkaline phosphatase (ALP), osteocalcin (OC), matrix metalloproteinase-1 (MMP-1), tissue inhibitor of metalloproteinase-1 (TIMP-1), osteoprotegerin (OPG) and receptor activator of NF- κ B ligand (RANKL). Ct values were normalized to the housekeeping gene hypoxanthine guanine phosphoribosyltransferase (HPRT). Primer sequences are shown in Table I. Polymerase chain reaction was performed following the manufacturer's instructions per the following process: 95°C for two minutes, 40 cycles of 95°C for five seconds, and 65°C for 25 seconds. For further analyses, the $\Delta\Delta$ Ct method was applied. The relative expression of each target mRNA was normalized to the housekeeping gene according to the equation: Δ Ct = Ct_{target} - Ct_{HPRT}. The relative amount of target mRNA of unloaded samples and samples treated with micromotions was compared with the mRNA level of the loaded control using the equation $\Delta\Delta$ Ct = Δ Ct_{unloaded control/micromotion} - Δ Ct_{loaded control}. For the expression ratio of the bone remodelling markers the following equation was used: $\Delta\Delta$ Ct = Δ Ct_{OPG/TIMP-1} - Δ Ct_{RANKL/MMP-1}.

The resulting gene expression is presented as the 2^{- $\Delta\Delta$ Ct} value.

Propeptide of pro-collagen type I was measured in cell culture supernatant as a measure of Col I synthesis using the enzyme-linked immunosorbent assay (ELISA) (MicroVue C1CP EIA; Quidel Corporation, San Diego, California).

For quantification of ALP activity, osteoblasts were washed twice with Tris-buffered saline and lysed in distilled water containing 1% Triton X and 1% phenyl-methylsulfonyl fluoride (PMSF) for ten minutes at room temperature. Cell lysates were incubated with 1 mM p-nitrophenyl phosphate (PNPP), 100 mM 2-amino-2-methyl-1-propanol, and 5 mM magnesium chloride (MgCl₂) in distilled water for one hour at 37°C, and absorbance of the solution was detected at 405 nm in a microplate reader (Tecan Group Ltd, Männedorf, Switzerland).

Data illustration and statistical analysis. Each test was conducted with osteoblasts obtained from six patients. Data are depicted as box plots showing the median, 25th and 75th percentile, and minimum and maximum. Values for metabolic activity, ALP activity, and pro-collagen type I were normalized to relative live cell counts. Data of unloaded samples and samples dedicated to micromotions were compared with loaded controls and are depicted as fold change. The statistical testing was done with GraphPad Prism 7 (GraphPad Software, La Jolla, California). Differences to loaded controls were statistically analyzed using Wilcoxon's signed-rank test. Differences between different treatment groups were analyzed using the Kruskal-Wallis test and Dunn's multiple comparison Test. The level of significance was set to $p < 0.05$.

Results

Influence of micromotions on viability of human osteoblasts. In unloaded samples, human osteoblasts grew confluent on top of the collagen material. Compared with the unloaded group, cell confluence on the collagen surface was reduced in loaded samples and appeared lowest in samples dedicated to micromotions (Fig. 3a). Living cell numbers were quantified after collagenase digestion of the collagen material (Fig. 3b). Loading of osteoblasts did not change the amount of living cells compared with unloaded samples. However, significantly higher live cell counts were found after loading and additional application of 25 μ m sine (1.28-fold) and 50 μ m triangle micromotions (1.32-fold, both $p = 0.0313$), but not after 50 μ m sine or 100 μ m sine micromotions, compared with loaded controls. Dead cells were also quantified by evaluation of fluorescent images (Fig. 3b). In unloaded samples, significantly fewer dead cells were detected compared with loaded samples (0.58-fold, $p = 0.0039$). As with live cell counts, the numbers of dead cells were significantly higher after 25 μ m sine (1.45-fold) and 50 μ m triangle micromotions (1.27-fold) compared with loaded controls (both $p = 0.0313$). Furthermore, the differences between

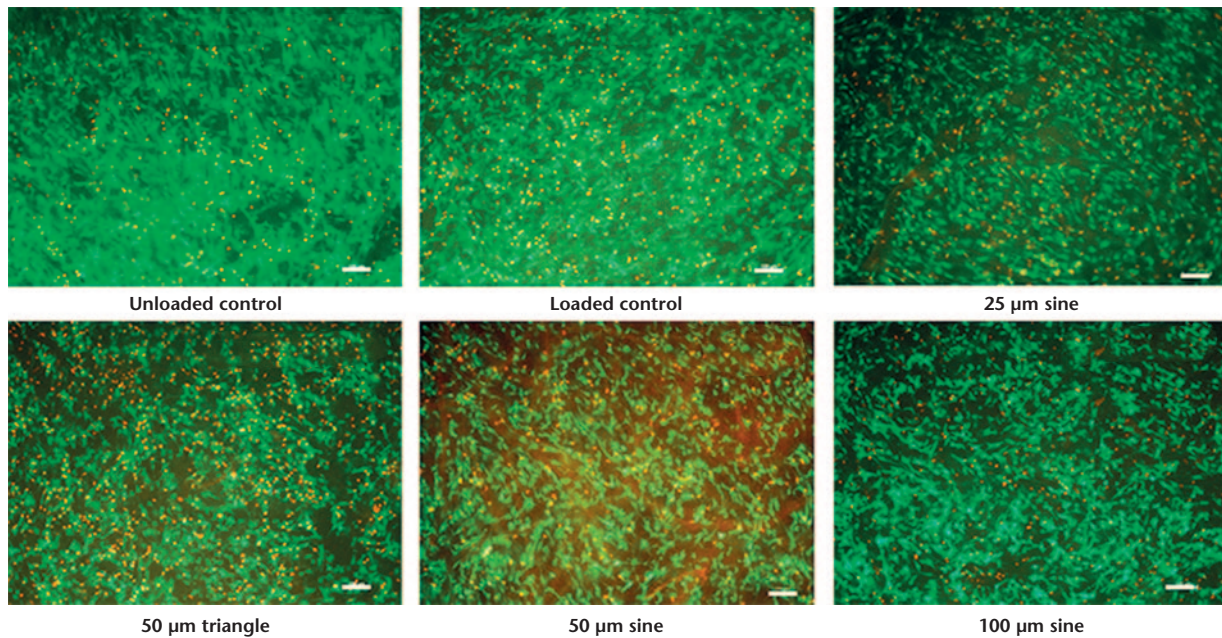


Fig. 3a

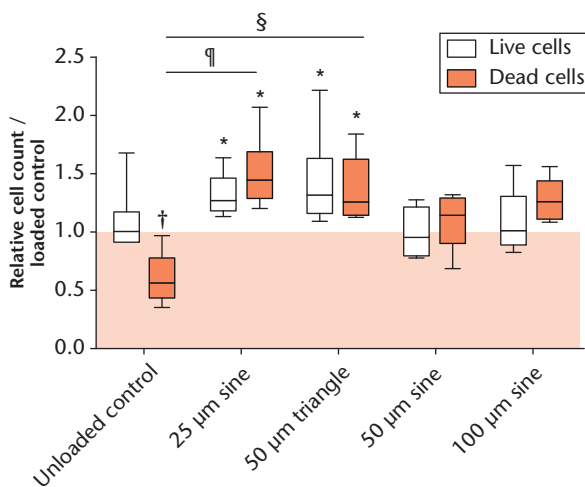


Fig. 3b

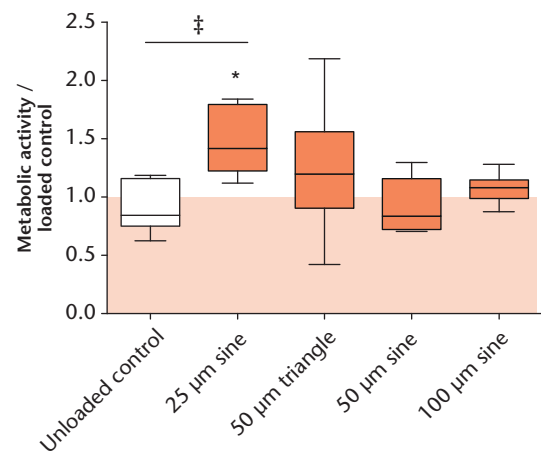


Fig. 3c

Cell viability of human osteoblasts: a) Live/Dead staining of osteoblasts growing on collagen material. Live cells appear green; nuclei of dead cells fluoresce red; white bar represents 100 μm . b) Graph showing the relative cell count of live and dead cells in unloaded samples and samples treated with micromotions compared with loaded controls. c) Graph showing the metabolic activity of osteoblasts in unloaded samples and samples treated with micromotions compared with loaded controls. * $p < 0.05$, † $p < 0.01$ compared with loaded control (Wilcoxon's signed-rank test); ‡ $p < 0.05$, § $p < 0.01$, ¶ $p < 0.001$ comparison between different groups (Kruskal–Wallis test and Dunn's multiple comparison test).

unloaded samples and 25 μm sine ($p = 0.0004$), as well as unloaded samples and the 50 μm triangle micromotion group ($p = 0.0081$), were statistically significant. The metabolic activity of osteoblasts (Fig. 3c) was significantly higher in samples treated with 25 μm sine micromotions compared with loaded controls (1.41-fold, $p = 0.0313$). The comparison of treatment groups further showed a significant difference between the unloaded control and 25 μm sine micromotions ($p = 0.0176$).

Influence of micromotions on expression of osteogenic markers. Gene expression analysis, depicted in Figure 4a, showed a significantly lower expression of COL1A1

in osteoblasts after treatment with micromotions, compared with loaded controls, reaching significance when treated with 50 μm triangle (0.43-fold) and sine micromotions (0.69-fold, both $p = 0.0313$). Alkaline phosphatase expression was slightly higher after 25 μm sine micromotions compared with loaded controls (1.18-fold). Osteocalcin expression was significantly upregulated during treatment with 25 μm sine micromotions compared with loaded controls (1.67-fold, $p = 0.0053$). With respect to protein levels, Col I synthesis (Fig. 4b) was highest in unloaded samples, showing a significantly higher synthesis rate (2.04-fold) compared with

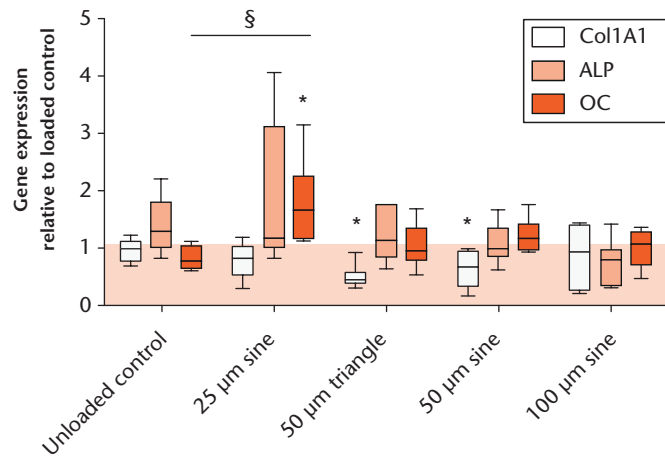


Fig. 4a

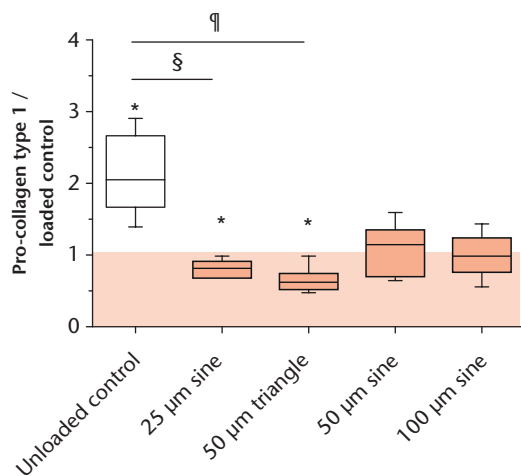


Fig. 4b

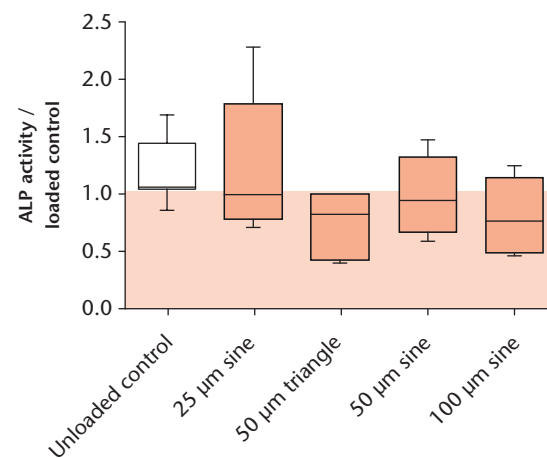


Fig. 4c

Expression of osteogenic markers in human osteoblasts: a) fold change of osteogenic genes collagen type I (COL1A1), alkaline phosphatase (ALP) and osteocalcin (OC); b) pro-collagen type I synthesis; and c) ALP activity of unloaded osteoblasts and osteoblasts treated with micromotions normalized to loaded samples (* $p < 0.05$ compared with loaded control (Wilcoxon's signed-rank test); § $p < 0.01$, ¶ $p < 0.001$ comparison between different groups (Kruskal–Wallis test and Dunn's multiple comparison test).

the loaded controls ($p=0.0313$). In line with the gene expression data, the Col I synthesis was significantly lower after 25 µm sine (0.80-fold) and 50 µm triangle micromotions (0.65-fold) compared with loaded controls (both $p=0.0313$). The multiple comparison of unloaded samples and micromotion groups showed significant differences between the unloaded control and 25 µm sine micromotions ($p=0.0096$) and the unloaded control and 50 µm triangle micromotions ($p=0.0001$). The ALP activity of osteoblasts was not significantly affected by the loading or micromotions (Fig. 4c).

Influence of micromotions on bone remodelling. Expression of TIMP-1 was 10^3 to 10^4 times higher than MMP-1 expression in all samples (Fig. 5a). No significant changes in gene expression were detected while comparing all groups. The OPG expression compared with the RANKL expression was highest in unloaded samples (9.03-fold, Fig. 5b). Static loading alone, as well as treatment with micromotions, decreased the OPG:RANKL expression ratio. The OPG:

RANKL expression ratio was significantly lower after 25 µm sine (0.90-fold, $p=0.036$) and 50 µm triangle (0.61-fold, $p=0.013$) micromotions, compared with OPG:RANKL expression in unloaded controls.

Discussion

We showed that 25 µm sine and 50 µm triangle micromotions applied with a velocity of 100 µm/s or less resulted in significantly higher numbers of osteoblasts being associated with higher numbers of detectable dead cells. The highest metabolic activity of human osteoblasts was found when 25 µm micromotions were applied. Live cell counts and metabolic activity were not significantly lower after the application of micromotions compared with the loaded and unloaded control, showing that the applied mechanical strains were not too extensive for the viability and proliferation of osteoblasts. However, smaller numbers of osteoblasts were visible on the collagen scaffolds in the fluorescent staining of living

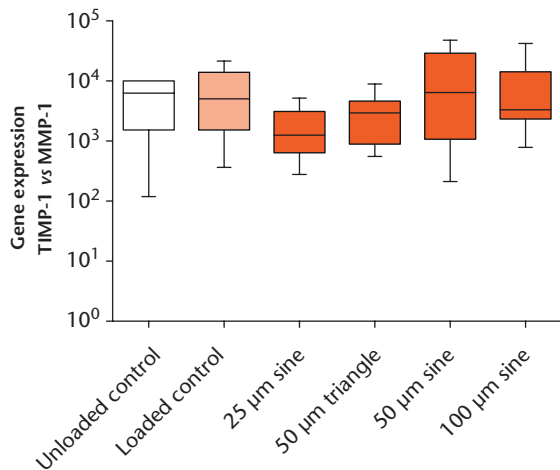


Fig. 5a

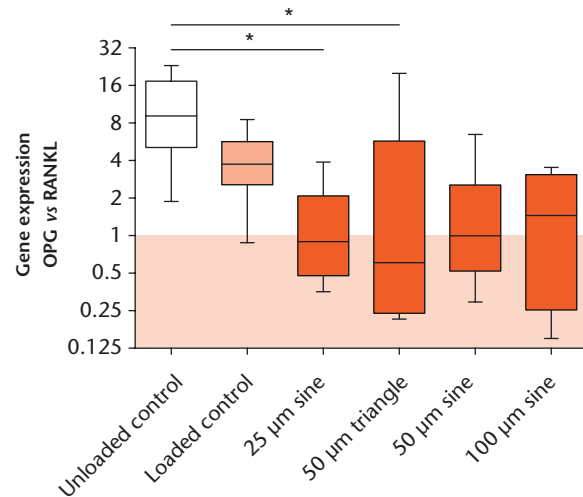


Fig. 5b

Expression of genes responsible for bone remodelling in human osteoblasts: a) fold change of tissue inhibitor of metalloproteinase-1 (TIMP-1) versus matrix metalloproteinase-1 (MMP-1); and b) osteoprotegerin (OPG) versus receptor activator of NF- κ B ligand (RANKL) in unloaded and loaded osteoblasts and osteoblasts treated with micromotions ($*p < 0.05$ comparison between different groups (Kruskal–Wallis test and Dunn's multiple comparison test). The colours correspond with the extent of strain exerted on the cells: unloaded control (white), no strain exerted on the cells; loaded control (light orange), affected by the static loading; micromotion (dark orange), strain on the cells (loading and micromotions).

cells after the loading and application of micromotions. Therefore, we hypothesize that the mechanical strain induces migration of osteoblasts into the collagen material and inhibits confluent growth on the surface of the scaffolds. The expression of osteogenic genes was also altered by micromotions, resulting in lower Col I synthesis after 25 μ m sine and 50 μ m triangle micromotions. Increased OC expression was detected with 25 μ m sine micromotions. Additionally, the OPG:RANKL ratio was decreased by the applied micromotions, indicating that bone remodelling might be influenced by micromotions via the promotion of bone resorption by facilitating osteoclast activation.⁵ In contrast, no significant differences were found in the ratio of the gene expression of TIMP-1 and MMP-1 between the experimental groups. In all groups, TIMP-1 expression was clearly higher than MMP-1 expression, indicating that collagen matrix is protected from degradation. However, TIMP-1 protein and phosphorylation of MMP-1 protein, which determines the activity of the enzyme, were not investigated, which represents a limitation of this study.

In our study, different effects could be observed when 50 μ m micromotions were applied with the same frequency but as sine or triangle signals. Discriminating between sine and triangle signals involves the limitation that each triangle signal can be decomposed into its frequency-dependent sine and cosine fractions according to the Fourier transform. Since the amplitudes of the harmonics with frequencies higher than 1 Hz are at least ten times smaller than the amplitude of the first harmonic at 1 Hz, we assumed that the effects of these on the cells are comparably low. The main difference between the 50 μ m triangle and sine signal is that the triangle waveform

results in a smaller maximum velocity and acceleration compared with the sine waveform, and therefore applies shear stress that is more similar to 25 μ m sine micromotions. It demonstrates that the effects of micromotions are likely due to the applied velocities and acceleration forces that operate on the cells and that result from the signal form and applied frequency, and not only from the magnitude of the micromotions. Since the piezo positioning system used here is limited to 100 μ m, higher shear stress can be achieved by increasing the frequency.

Pioletti et al²³ applied a comparable pressure of 500 Pa to MG-63 osteoblast-like cells and investigated the effects of 10 μ m sine micromotions applied with 1 Hz continuously for 24 hours. While the cell viability of osteoblasts was not affected by loading or micromotions, expression of osteogenic markers COL1A1, OC, and osteonectin was reduced by loading. An additional application of 10 μ m micromotions elevated the expression of osteogenic genes compared with loading alone, especially in the case of osteocalcin; its expression even reached the level of the unloaded controls after micromotion application.²³ Another study applied cyclic micromotions ranging from 0 μ m to 1000 μ m with a pressure load of 23 Pa and a frequency of 13 Hz to osteoblasts and found reduced metabolic and ALP activity.²⁴ Negative effects are likely to result from high velocities occurring from stimulation with 13 Hz and high amplitudes of micromotions. The application of 100 μ m with 1 Hz in our study did not affect metabolic and ALP activity. These findings indicate that small micromotions stimulate osteoblast differentiation and thereby promote osseointegration whereas higher micromotions interfere with bone formation.

As in other studies, the application of micromotions involved the application of a certain pressure to model an interface between bone cells and the implant. Therefore, the effects of loading, as well as the synergistic effects of loading and micromotions, were investigated but micromotions alone were not. The polished surface of the Ti6Al4V cylinders is a limitation of our study, as cementless implants have a rough surface for initial implant fixation into the surrounding bone tissue, appropriate ingrowth of bone, and an optimal force transfer.^{25,26} Depending on implant design and structure, strains at the bone-implant interface vary during application of micromotions and give rise to areas that permit or restrict bone growth.²⁷ Moreover, our system is not able to apply dynamic loading of the samples, and the loading forces are much smaller than those exerted on the bone tissue by the implant during the gait cycle *in vivo*.²⁸ Nevertheless, the combination of a defined static pressure and a range of micromotions exerting shear stress with varying velocities and accelerations was able to elicit specific cell reactions. The beneficial effects of small micromotions on osteoblast activity could be confirmed, while 50µm and 100µm sine micromotions had no impact or only a slight negative impact on osteoblast activity, being in line with literature stating that, *in vivo*, micromotions of 150µm, but not 20µm, induce extended fibrous tissue formation directly around an implant and thus impair osseointegration.¹⁶ The relationship between bone-implant contact and micromotions was also demonstrated on transverse sections of retrievals of uncemented hips under gait and stair-climbing test conditions.²⁹ It was also observed that micromotions alter osteoblast activity. However, it is not only the question of whether bone formation is taking place but also of how the bone is remodelled and the bone architecture altered in the implant periphery.³⁰ *In vivo* studies have shown that extended micromotions result in enhanced bone density surrounding the implant, forming a dense shell of bone separated from the implant by fibrous tissue – a situation associated with reduced implant stability when observed in radiographs. Bone remodelling might be induced by microfractures and high stresses appearing during progressive micromotions.^{16,19}

In future studies, Ti6Al4V specimens will be modified so that surfaces varying in geometry and roughness can be tested. Furthermore, different bone substitute materials and composites, such as seeding substrate, can be used instead of collagen material to further approach physiological conditions. It is also planned to model more complex motion sequences with the respective acceleration forces associated with walking or stair-climbing. Sine and triangle waveforms are ideal harmonic oscillations, but do not comply with the more stochastic oscillations we assume at the bone-implant interface.

In summary, we presented a system that enables the investigation of bone cell behaviour at the bone-implant

interface under micromotion-induced shear stress. Osteoblasts cultured on collagen scaffolds were strongly affected by 25µm sine and 50µm triangle micromotions, resulting in enhanced numbers of living and dead cells and reduced Col I synthesis. Micromotions of 25µm further increased metabolic activity and gene expression of osteocalcin.

References

1. Takenaga RK, Callaghan JJ, Bedard NA, et al. Cementless total hip arthroplasty in patients fifty years of age or younger: a minimum ten-year follow-up. *J Bone Joint Surg [Am]* 2012;94-A:2153-2159.
2. Wyatt M, Hooper G, Frampton C, Rothwell A. Survival outcomes of cemented compared to uncemented stems in primary total hip replacement. *World J Orthop* 2014;5:591-596.
3. Brånemark PI. Osseointegration and its experimental background. *J Prosthet Dent* 1983;50:399-410.
4. Mavrogenis AF, Dimitriou R, Parvizi J, Babis GC. Biology of implant osseointegration. *J Musculoskelet Neuronal Interact* 2009;9:61-71.
5. Fillingham Y, Jacobs J. Bone grafts and their substitutes. *Bone Joint J* 2016;98-B(Suppl A):6-9.
6. Alm JJ, Moritz N, Aro HT. *In vitro* osteogenic capacity of bone marrow MSCs from postmenopausal women reflect the osseointegration of their cementless hip stems. *Bone Rep* 2016;5:124-135.
7. Feller L, Jadwat Y, Khammissa RA, et al. Cellular responses evoked by different surface characteristics of intraosseous titanium implants. *Biomed Res Int* 2015;2015:171945.
8. Sammons RL, Lumbikanonda N, Gross M, Cantzler P. Comparison of osteoblast spreading on microstructured dental implant surfaces and cell behaviour in an explant model of osseointegration. A scanning electron microscopic study. *Clin Oral Implants Res* 2005;16:657-666.
9. Sennerby L, Gottlow J, Meredith N, Fredrik E. Histological and biomechanical aspects of surface topography and geometry of neoss implants. A study in rabbits. *Appl Osseointegration Res* 2008;6:18-22.
10. Antoniadou G, Smith EJ, Deakin AH, Wearing SC, Sarungi M. Primary stability of two uncemented acetabular components of different geometry: hemispherical or peripherally enhanced? *Bone Joint Res* 2013;2:264-269.
11. Yamauchi R, Itabashi T, Wada K, et al. Photofunctionalised Ti6Al4V implants enhance early phase osseointegration. *Bone Joint Res* 2017;6:331-336.
12. Dimitriou R, Babis GC. Biomaterial osseointegration enhancement with biophysical stimulation. *J Musculoskelet Neuronal Interact* 2007;7:253-265.
13. Muderis MA, Tetsworth K, Khemka A, et al. The Osseointegration Group of Australia Accelerated Protocol (OGAAP-1) for two-stage osseointegrated reconstruction of amputated limbs. *Bone Joint J* 2016;98-B:952-960.
14. Søhalle K, Hansen ES, B-Rasmussen H, Jørgensen PH, Bünger C. Tissue ingrowth into titanium and hydroxyapatite-coated implants during stable and unstable mechanical conditions. *J Orthop Res* 1992;10:285-299.
15. Karl M, Graef F, Winter W. Determination of micromotion at the implant bone interface—an in-vitro methodologic study. *Dentistry* 2015;5:289.
16. Jasty M, Bragdon C, Burke D, et al. In vivo skeletal responses to porous-surfaced implants subjected to small induced motions. *J Bone Joint Surg [Am]* 1997;79-A:707-714.
17. Kawahara H, Kawahara D, Hayakawa M, et al. Osseointegration under immediate loading: biomechanical stress-strain and bone formation-resorption. *Implant Dent* 2003;12:61-68.
18. Szmukler-Moncler S, Salama H, Reingewirtz Y, Dubruille JH. Timing of loading and effect of micromotion on bone-dental implant interface: review of experimental literature. *J Biomed Mater Res* 1998;43:192-203.
19. Duyck J, Vandamme K, Geris L, et al. The influence of micro-motion on the tissue differentiation around immediately loaded cylindrical turned titanium implants. *Arch Oral Biol* 2006;51:1-9.
20. Malfroy Camine V, Terrier A, Pioletti DP. Micromotion-induced peri-prosthetic fluid flow around a cementless femoral stem. *Comput Methods Biomech Biomed Engin* 2017;20:730-736.
21. Kämmerer PW, Thiem DGE, Alshihri A, et al. Cellular fluid shear stress on implant surfaces—establishment of a novel experimental set up. *Int J Implant Dent* 2017;3:22.

22. **Jonitz A, Lochner K, Lindner T, et al.** Oxygen consumption, acidification and migration capacity of human primary osteoblasts within a three-dimensional tantalum scaffold. *J Mater Sci Mater Med* 2011;22:2089-2095.
23. **Pioletti DP, Müller J, Rakotomanana LR, Corbeil J, Wild E.** Effect of micromechanical stimulations on osteoblasts: development of a device simulating the mechanical situation at the bone-implant interface. *J Biomech* 2003;36:131-135.
24. **Lewandowska-Szumieł M, Sikorski K, Szummer A, et al.** Experimental model for observation of micromotion in cell culture. *J Biomed Mater Res B Appl Biomater* 2005;72:379-387.
25. **Yamada H, Yoshihara Y, Henmi O, et al.** Cementless total hip replacement: past, present, and future. *J Orthop Sci* 2009;14:228-241.
26. **Wiskott HW, Belser UC.** Lack of integration of smooth titanium surfaces: a working hypothesis based on strains generated in the surrounding bone. *Clin Oral Implants Res* 1999;10:429-444.
27. **Wazen RM, Currey JA, Guo H, et al.** Micromotion-induced strain fields influence early stages of repair at bone-implant interfaces. *Acta Biomater* 2013;9:6663-6674.
28. **Bergmann G, Deuretzbacher G, Heller M, et al.** Hip contact forces and gait patterns from routine activities. *J Biomech* 2001;34:859-871.
29. **Mann KA, Miller MA, Costa PA, Race A, Izant TH.** Interface micromotion of uncemented femoral components from postmortem retrieved total hip replacements. *J Arthroplasty* 2012;27:238-245.e1.
30. **Brunski JB.** In vivo bone response to biomechanical loading at the bone/dental-implant interface. *Adv Dent Res* 1999;13:99-119.

Acknowledgements

- The authors would like to thank Ms Ronja Dreger and Ms Katrin Szczygielski (Rostock University Medical Center, Rostock, Germany) for supporting the development of the *in vitro* system.

Funding Statement

- This work was funded by the International Team for Implantology (ITI) Foundation (grant no. 1107_2015).

Author Contributions

- J. Ziebart: Planning the experiments, Creating the figures, Writing the manuscript.
- S. Fan: Performing the experiments.
- C. Schulze: Supervising the construction and initial operation of the *in vitro* system, Providing technical support.
- P. W. Kämmerer: Writing the application for the financial funding of the project, Drafting the biological experiments.
- R. Bader: Providing the idea to investigate micromotions, Providing the scientific support for the construction of the *in vitro* system, Initiating the cooperation of the Department of Orthopaedics and Department of Oral, Maxillofacial and Plastic Surgery.
- A. Jonitz-Heincke: Writing the application for the financial funding of the project, Drafting the biological experiments, Supervising the cell experiments.

Conflicts of Interest Statement

- The authors state no conflicts of interest.

© 2018 Ziebart et al. This is an open-access article distributed under the terms of the Creative Commons Attribution licence (CC-BY-NC), which permits unrestricted use, distribution, and reproduction in any medium, but not for commercial gain, provided the original author and source are credited.